IV International Conference on Simulation for Additive Manufacturing
Sim-AM 2023
E. Rank and S. Kollmannsberger (Eds)

THERMAL AND MECHANICAL CALIBRATION OF MULTI-MATERIAL DED AM PROCESS SIMULATIONS ON PART-SCALE

JOS VROON*, ARJEN D. D. VAN DER EEMS* AND WOUTER M. VAN DEN BRINK*

* Royal Dutch Aerospace Centre (NLR)
Department of collaborative engineering
Anthony Fokkerweg 2, 1059 CM Amsterdam, The Netherlands
e-mail: jos.vroon@nlr.nl, web page: http://www.nlr.org

Key words: numerical simulations, Additive manufacturing (AM), computational modeling

Abstract. Additive Manufacturing (AM) processes, such as Directed Energy Deposition (DED), offer great potential for producing complex and customized components. To optimize these processes, accurate simulations and numerical modeling techniques are essential. This paper presents a study on the thermal and mechanical calibration of DED AM process simulations on a part-scale. The research aims to develop a comprehensive finite element model that incorporates the multi-physics nature of the DED process, accurately predicting thermal behavior, internal stresses, and distortion of manufactured components. The calibration process involves experimental measurements and simulations using Abaqus software. The thermal calibration involves calibrating parameters such as emissivity, absorptivity, and convection coefficients, while the mechanical calibration focuses on plastic strain properties. Additionally, the study explores the simulation of multi-material prints and functionally graded materials. The results demonstrate that the models can accurately represent thermal and mechanical phenomena, with calibration of material properties playing a crucial role. The paper concludes with recommendations for further validation, including demonstrator prints and investigations into simulation parameters. This research contributes to advancing the understanding and application of DED AM simulations, enabling more accurate and reliable predictions for industrial applications.

1 INTRODUCTION

Additive Manufacturing (AM), also known as 3D printing, has revolutionized the manufacturing industry by enabling the production of complex geometries and customized components with enhanced functionalities. One of the promising AM techniques is Directed Energy Deposition (DED), which involves the precise deposition of material layers using a focused energy source, such as a laser or an electron beam. DED offers numerous advantages, including the ability to repair, modify, or fabricate large-scale components with various materials, making it highly relevant for applications in aerospace, automotive, and medical industries.

To optimize the performance and reliability of DED processes, accurate simulations and

numerical modelling techniques are crucial. Finite Element Modelling (FEM) has emerged as a powerful tool for analysing and predicting the behaviour of complex systems, including AM processes. FEM enables the simulation of material deposition, heat transfer, and thermo-mechanical phenomena, providing insights into the process dynamics and aiding in the design and optimization of DED parameters.

Numerous studies have been conducted to explore finite element modelling of DED processes, with a focus on understanding the influence of process parameters on the resulting properties of manufactured components. For instance, Piscopo et al. [1] developed a finite element model specifically for simulating single tracks in DED. Their findings demonstrated excellent agreement with experimental measurements, thereby confirming the accuracy of the model. Similarly, Stender et al. [2] established a finite element workflow to investigate the DED additive manufacturing process. However, most research efforts have primarily concentrated on the single track or even melt pool scale. Kaini et al. [3] revealed that relying solely on single track parameters has limited scalability to bulk geometries. Consequently, there is a pressing need for numerical process models that encompass part-scale simulations to better understand DED on a larger scale.

While significant progress has been made in the field of finite element modelling of DED, there are still several challenges that need to be addressed. One of the key challenges is accurately capturing the complex interactions between the energy source, powder material, and substrate during the DED process. The multi-physics nature of the process, involving heat transfer, fluid flow, phase change, and mechanical deformation, necessitates the development of comprehensive and robust numerical models.

The primary objective of this technical paper is to develop and validate a finite element model for the simulation of the additive manufacturing method of DED. The model will consider the multi-physics nature of the process, accounting for thermal and mechanical phenomena. By accurately capturing the underlying physics, the model will enable the prediction of residual stresses and distortion of the manufactured components. The nature of DED can be described as the process in which a small melt pool with very complex physics builds a large part over time. To accurately incorporate all physics of the melt pool a high level of detail is essential. This high level of detail results in very large high fidelity models that will not be able to simulate a complete part. This paper will focus on part-scale simulations that will simplify the complex physics of the melt pool. These part-scale simulations shall then be experimentally calibrated.

This paper is structured into several sections. Section 2 provides a detailed description of the materials and methods employed in the study, focusing on the thermal and mechanical models, which are discussed separately. Section 3 presents and discusses the results obtained from the experiments and simulations. The paper concludes with the findings, recommendations, and conclusions in section 4.

2 MATERIALS AND METHODS

This section outlines the methods employed to investigate DED AM processes, with all simulations conducted using Abaqus software. The simulations are structured as sequential thermal and mechanical analyses. In the initial step, a thermal simulation is performed. This simulation incorporates machine parameters, such as laser power, speed, and toolpath, along

with thermal parameters including conduction coefficients, convection coefficients, emissivity, absorptivity, and ambient temperature. These inputs collectively generate a step-by-step temperature field across the entire print. The temperature field obtained from the thermal simulation serves as the input for the subsequent mechanical simulation. The mechanical simulation incorporates material properties, such as Young's moduli, coefficient of thermal expansion, and plastic strain. Through these inputs, the mechanical simulation calculates internal stresses and resulting distortions. By employing this two-step simulation approach, it becomes possible to analyse the thermal and mechanical behaviour of the DED AM process comprehensively. There are three distinct models that have been analysed. The models are a thermal calibration model, a mechanical calibration model and a mechanical multi material calibration model. These models are described in their own three subchapters.

The simulation setup typically involves the following steps. Firstly, the entire geometry to be printed, including its surroundings, is defined and incorporated into the simulation. During the simulations, the material that is to be printed remains inactive until it encounters an "event box" passing through the material elements. This event box is characterized by specific properties, such as size, shape, and other relevant attributes. Additionally, it is assigned a toolpath derived from G-code instructions used for the actual printing process. The thermal simulations establish a coupling between the event box and a laser spot, which governs the heat input into the material elements. The resulting temperatures are recorded and subsequently utilized in the mechanical simulation to calculate thermal shrinkage and deformation. Figure 1 provides a visual representation of the event box. By incorporating these steps, the simulations effectively model the heat transfer and resulting mechanical behaviour during the DED AM process.

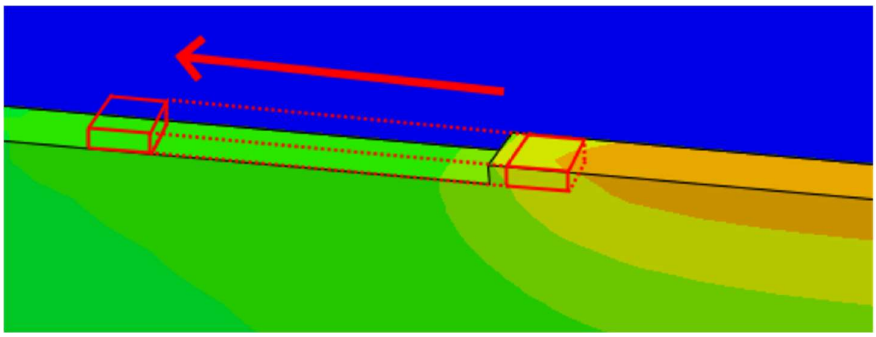

Figure 1: Representation of the event box that is used in the AM simulations. This box represent the location at which the machine is adding material and heat.

2.1 Thermal experiment and simulation

In order to calibrate the thermal parameters of the model, a specialized print was created and simulated. This print comprised four single track walls, each employing different printing strategies (e.g., left-to-right or zig-zag). One of the walls was equipped with thermocouples to directly measure temperatures, while all walls were recorded using a thermal camera. To establish a consistent emissivity value for the camera calibration, one of the walls was painted black. Subsequently, all four walls were doubled in height by adding additional material on top, and temperature measurements were recorded. These measurements were then utilized to calibrate the material properties of the model. The calibration process ensures that the simulated

temperature distribution and thermal behaviour align with the experimental measurements, improving the accuracy and reliability of the model's thermal predictions.

The DED AM process involves numerous parameters, and their precise values may vary in terms of availability and accuracy. Table 1 presents the material properties utilized in the model, which are sourced from existing literature and have not been calibrated for this specific study. However, there are certain parameters in the thermal model that require calibration. These include the absorptivity, convection coefficients, and emissivity coefficients. Calibrating these parameters is crucial for achieving accurate thermal predictions in the model, as they directly impact the heat transfer and temperature distribution during the printing process.

Table 1: Temperature dependent material properties for SS316L that are used in the thermal modelling.

Temperature [°C]	conductivity [W/m K]	Density [kg/m^3]	Young's modulus [Pa]	Poisson's ratio [-]	CTE [-]	Specific heat [J/kg K]
20	14.12	7966	1.96E+11	0.294	1.46E-05	492
100	15.26	7966	1.91E+11	0.294	1.54E-05	502
200	16.69	7966	1.86E+11	0.294	1.62E-05	514
300	18.11	7966	1.80E+11	0.294	1.69E-05	526
400	19.54	7966	1.73E+11	0.294	1.74E-05	538
500	20.96	7966	1.65E+11	0.294	1.78E-05	550
600	22.38	7966	1.55E+11	0.294	1.81E-05	562
700	23.81	7966	1.41E+11	0.294	1.84E-05	575
800	25.23	7966	1.31E+11	0.294	1.87E-05	587
900	26.66	7966	1.17E+11	0.294	1.90E-05	599
1000	28.08	7966	1.00E+11	0.294	1.93E-05	611
1100	29.5	7966	8.00E+10	0.294	1.95E-05	623
1200	30.93	7966	5.70E+10	0.294	1.98E-05	635
1300	32.35	7966	3.00E+10	0.294	2.00E-05	647
1400	33.78	7966	2.00E+09	0.294	2.02E-05	659

2.2 Mechanical experiment and simulation

To calibrate the mechanical model, a specific print was required to exhibit predictable deformation. While cantilevers are commonly used for this purpose in Laser Powder Bed Fusion (LPBF), the design of LPBF cantilevers was not suitable for the DED process. However, a similar principle was adopted. It was observed that when prints were made on a thin base plate, the base plate would deform in response. This observation was leveraged to create a print that would deform in a controlled manner. A slotted base plate was utilized and several thick walls were subsequently printed on top of it (as depicted in Figure 3). These additional structures induced an upward distortion of the base plate. The size, laser speed, and power of the printed walls were varied to examine their effects on the resulting distortion. By manipulating these variables, it becomes possible to study and calibrate the mechanical model to accurately predict the distortion behaviour exhibited by the prints.

In addition to the properties listed in Table 1, the mechanical model incorporates several other parameters, with the plastic strain properties of the material being particularly notable. Initial tests indicated that these parameters play a critical role in achieving accurate results. The specific plastic strain parameters utilized in the model are provided in Table 2. These parameters capture the material's response to plastic deformation and are essential for accurately predicting the mechanical behaviour and response of the printed components.

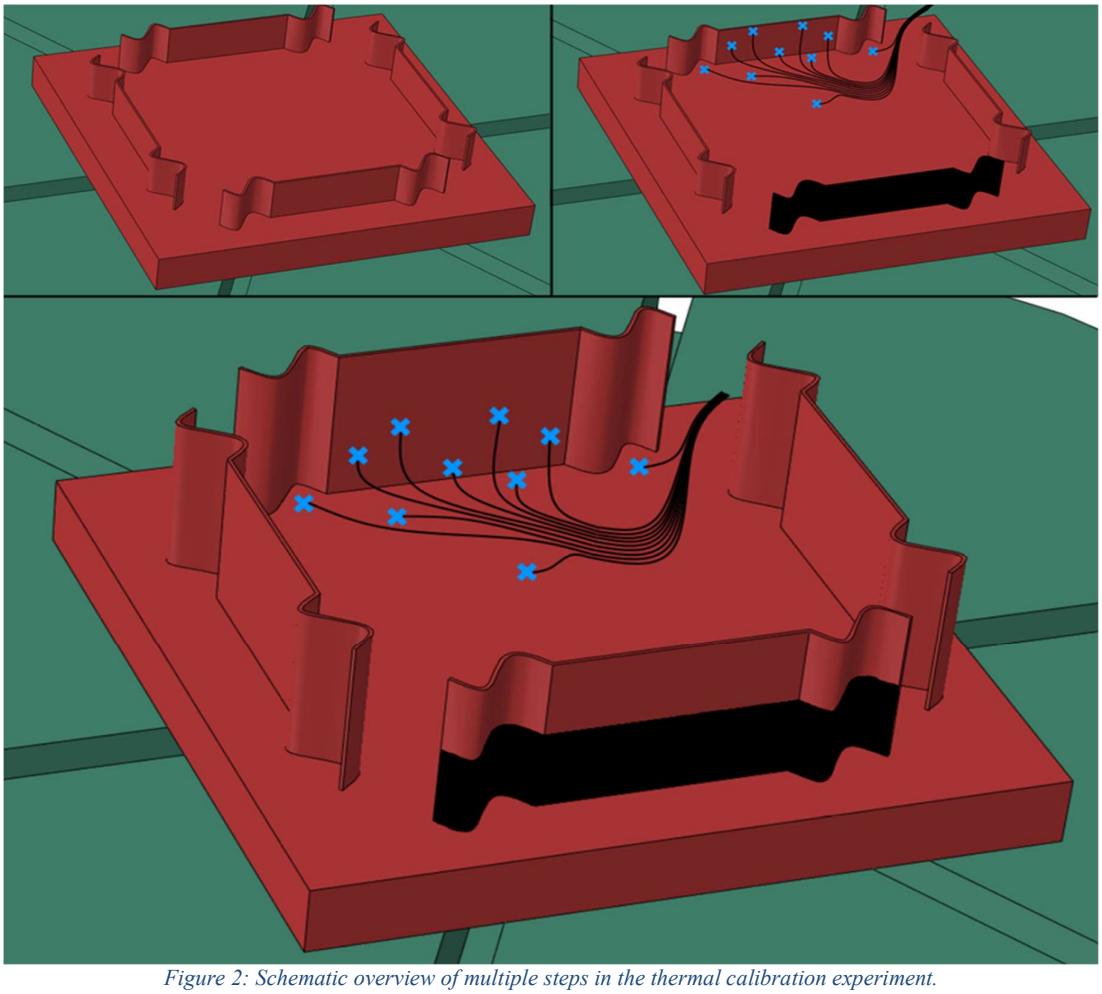

Figure 2: Schematic overview of multiple steps in the thermal calibration experiment.

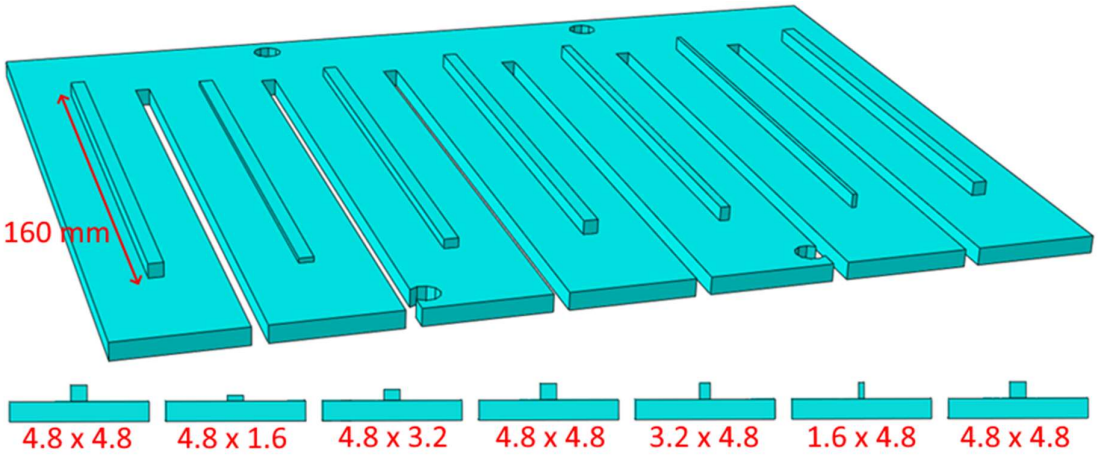

Figure 3: The design for the cantilevers to be printed with DED.

Table 2: Temperature and strain dependant plasticity material property for SS316L. Values are given in MPa. [4]

Strain [-]	0	0.002	0.01	0.02	0.05	0.1	0.2	0.3	0.4
23 °C	210	238	292	325	393	494	648	775	880
275 °C	150	173.7	217	249	325	424	544	575	575
550 °C	112	142.3	178	211	286	380	480	500	500
750 °C	95	114.7	147	167	195	216	231	236	236
800 °C	88	112	120	129	150	169	183	183	183
900 °C	69	70	71	73	76	81	81	81	81
1100 °C	22	22	22	22	22	22	22	22	22
1400 °C	5	5	5	5	5	5	5	5	5

2.3 Mechanical multi-material experiment and simulation

One of the intriguing aspects of DED is its versatility in printing with different materials. This includes the ability to create material gradients by combining different powders within a single powder flow (as shown in Figure 5). To examine whether the modelling technique can effectively capture the effects of different materials and material gradients, the cantilever print is replicated using multiple materials. Instead of varying the dimensions of the walls, this print involves the use of different materials. Specifically, the materials employed are SS316L and Inconel. These materials are combined to form bimetal structures or are blended to create functionally graded materials (as depicted in Figure 4). This experimental setup allows for the investigation of how the modelling technique captures the behaviour and performance of prints composed of multiple materials and material gradients.

The material properties for Inconel utilized in the analysis are provided in Table 3. Additionally, the plastic strain parameters for Inconel are given in Table 4. In the case of material gradients, the material properties are linearly interpolated to account for the varying composition throughout the gradient. This interpolation ensures that the mechanical model captures the changing material properties and their impact on the structural behaviour of the printed components.

Table 3: Temperature dependent material properties for Inconel that are used in the thermal modelling.

Temperature [°C]	Conductivity [W/m K]	Density [kg/m^3]	Young's modulus [Pa]	Poisson's ratio [-]	CTE [-]	Specific heat [J/kg K]
20	9.94	8190	2.00E+11	0.3	1.34E-05	420
100	11.59	8190	1.93E+11	0.3	1.41E-05	440
200	13.24	8190	1.87E+11	0.3	1.47E-05	460
300	14.91	8190	1.84E+11	0.3	1.53E-05	480
400	16.61	8190	1.78E+11	0.3	1.57E-05	500
500	18.34	8190	1.71E+11	0.3	1.68E-05	520
600	19.8	8190	1.63E+11	0.3	1.79E-05	580
700	21.26	8190	1.54E+11	0.3	1.90E-05	630
800	22.72	8190	1.52E+11	0.3	2.01E-05	630
900	23.61	8190	1.30E+11	0.3	2.12E-05	630
1000	24.47	8190	1.10E+11	0.3	2.19E-05	630
1100	25.32	8190	9.86E+10	0.3	2.25E-05	630

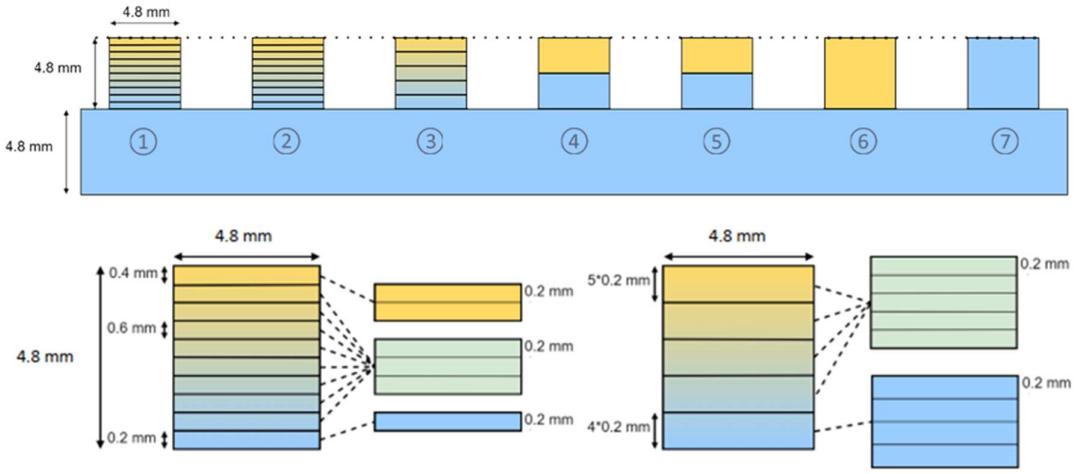

Figure 4: Cantilever design for the multi-material print and model. Blue represents SS316L, yellow represents Inconel and green represents gradient steps with both materials in a certain combination.

Table 4: Temperature and strain dependant plasticity material property for Inconel. Values are given in MPa. [5]

Strain [-]	**0**	**0.05**	**0.1**	**0.2**	**0.3**	**0.4**
20 °C	649	852	936	1074	1203	1302
300 °C	481	699	852	1011	1136	1220
550 °C	481	712	813	953	1074	1184
850 °C	397	470	507	556	602	640
1000 °C	289	321	364	382	388	386

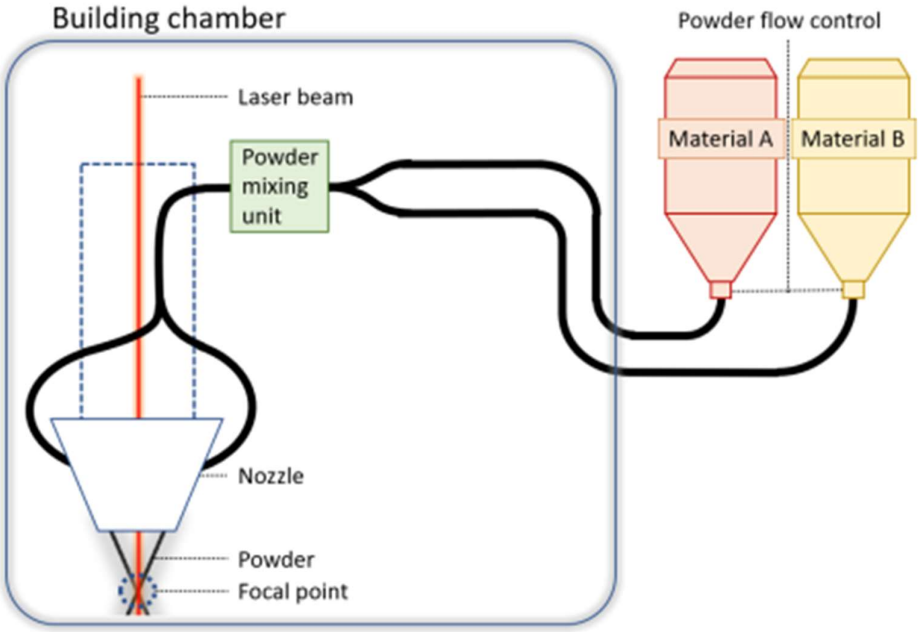

Figure 5: Schematic view of the mechanism for combining the flows of material powders to create graded materials.

3 RESULTS AND DISCUSSION

The results are presented in a manner that follows the order of the methods described. Firstly, the thermal calibration results are provided, followed by the mechanical calibration results. Lastly, the findings from the multi-material calibration are presented. This organization allows for a coherent and structured presentation of the research outcomes, facilitating clear and logical discussions for each aspect of the study.

3.1 Thermal calibration

The results of the thermal calibration are illustrated in Figure 6 and Figure 7. The initial step involves utilizing data from the thermal camera to calibrate the emissivity value. By filming the black wall with a known emissivity, it becomes possible to calibrate the emissivity of a regular wall and compare the data. Figure 6 demonstrates that the emissivity of the printed material is approximately 0.45, as determined through the calibration process. This calibrated emissivity value is crucial for accurate temperature measurements during the thermal simulations.

Subsequently, the calibrated emissivity value is incorporated into the models, and the other thermal parameters are then calibrated. These parameters include the absorptivity, emissivity of the base, convection constant of the print, and convection constant of the base. The absorptivity primarily affects the height of the thermal peaks, while the other three parameters impact the cooldown ramp after printing. The results of the thermal parameter calibration are summarized in Table 5. This table presents the calibrated values for each parameter, providing important information for accurately simulating the thermal behaviour during the DED AM process.

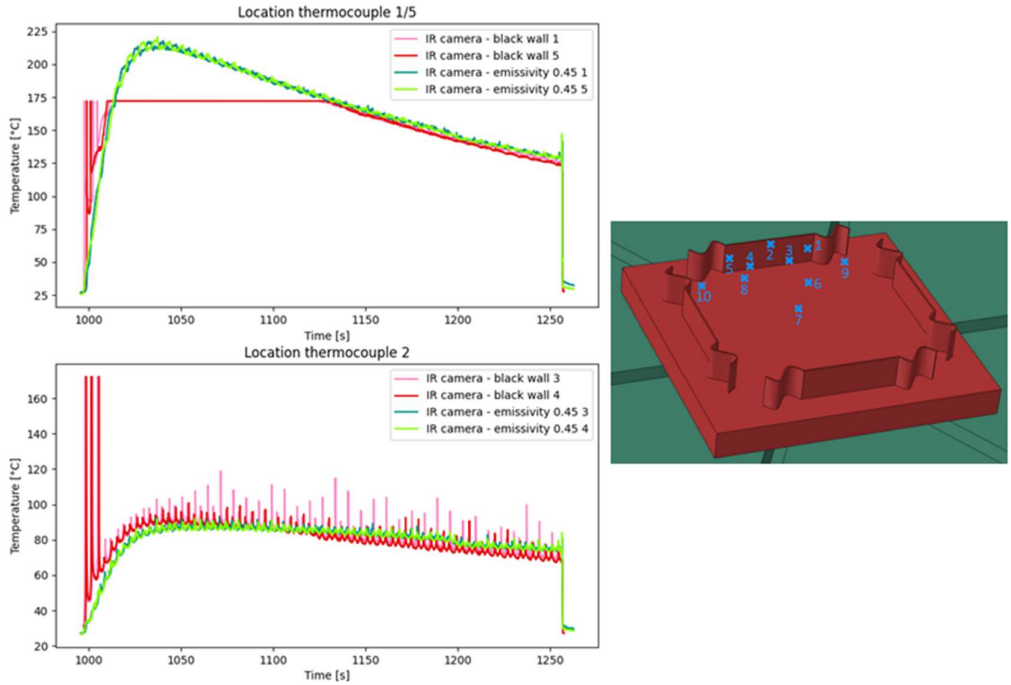

Figure 6: [left] Comparison of the blackened wall and a regular wall with calibrated emissivity value. Note that the measurements of the IR camera are cut-off at a maximum, this is due to the camera settings. [Right] Locations of the thermocouples on the print.

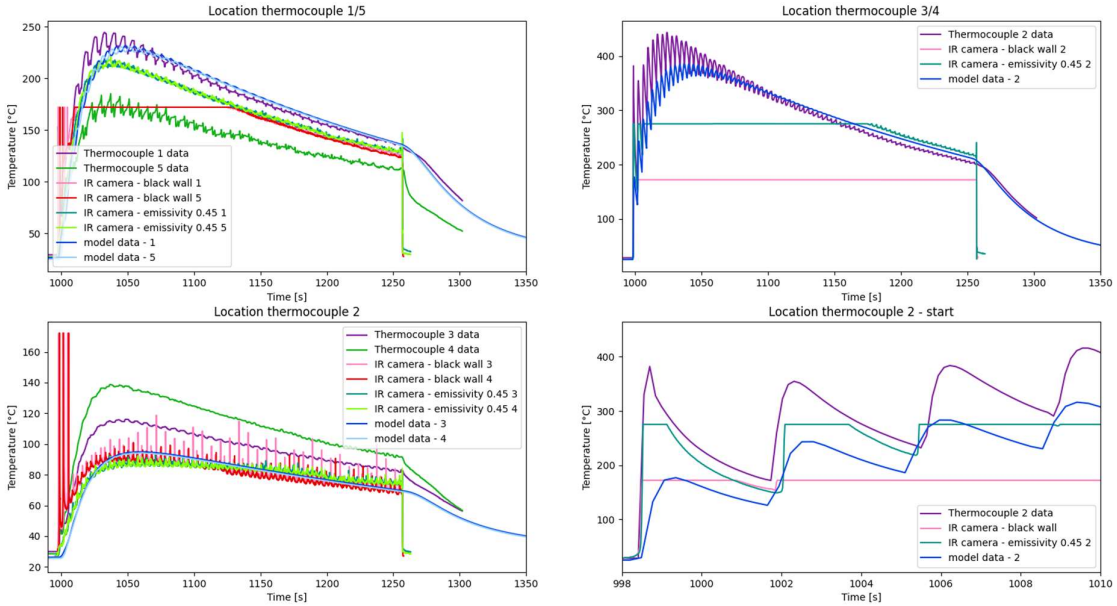

Figure 7: Result of the measurements of the thermal calibration prints and model data with calibrated values. Note that the measurements of the IR camera are cut-off at a maximum, this is due to the camera settings.

Table 5: Result of the thermal calibration.

Absorptivity [-]	0.3
Convection constant (printed part) [W/m^2 K]	25
Convection constant (base) [W/m2 K]	10
Emissivity constant (printed part) [-]	0.45
Emissivity constant (base) [-]	0.3

3.2 Mechanical calibration

The results of the mechanical calibration are presented in Figure 8, Figure 9, and Figure 10. Figure 8 visually displays the deformed cantilevers, showcasing that the cantilever principle effectively induced the desired distortion. This confirms the successful calibration of the mechanical model. Figure 9 demonstrates that the FE model accurately replicates the distortion observed in the physical print. The simulated distortion exhibits the same direction and magnitude as the physical print, validating the accuracy and reliability of the FE model in capturing the mechanical behaviour of the printed components. These results signify the successful calibration of the mechanical model, indicating that it can effectively predict the distortion and deformation patterns of the printed structures.

The results of the actual deformation, as well as the results for the multi-material prints, are discussed in the subsequent subchapter. This consolidated discussion allows for a comprehensive examination of the deformation patterns observed in both the single-material and multi-material prints. By analysing these results together, a deeper understanding of the effects of material composition and gradients on the deformation behaviour of the printed was gained.

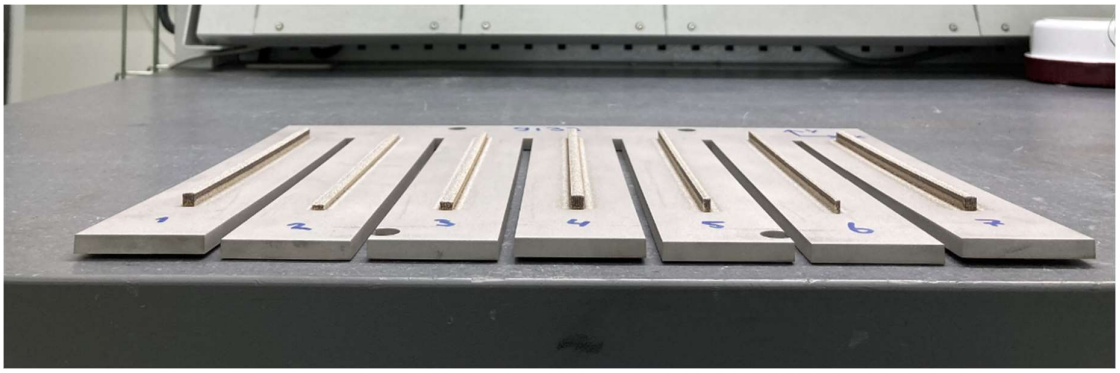

Figure 8: Picture of the deformed cantilever print. Note how different geometries of the printed walls result in different distortions.

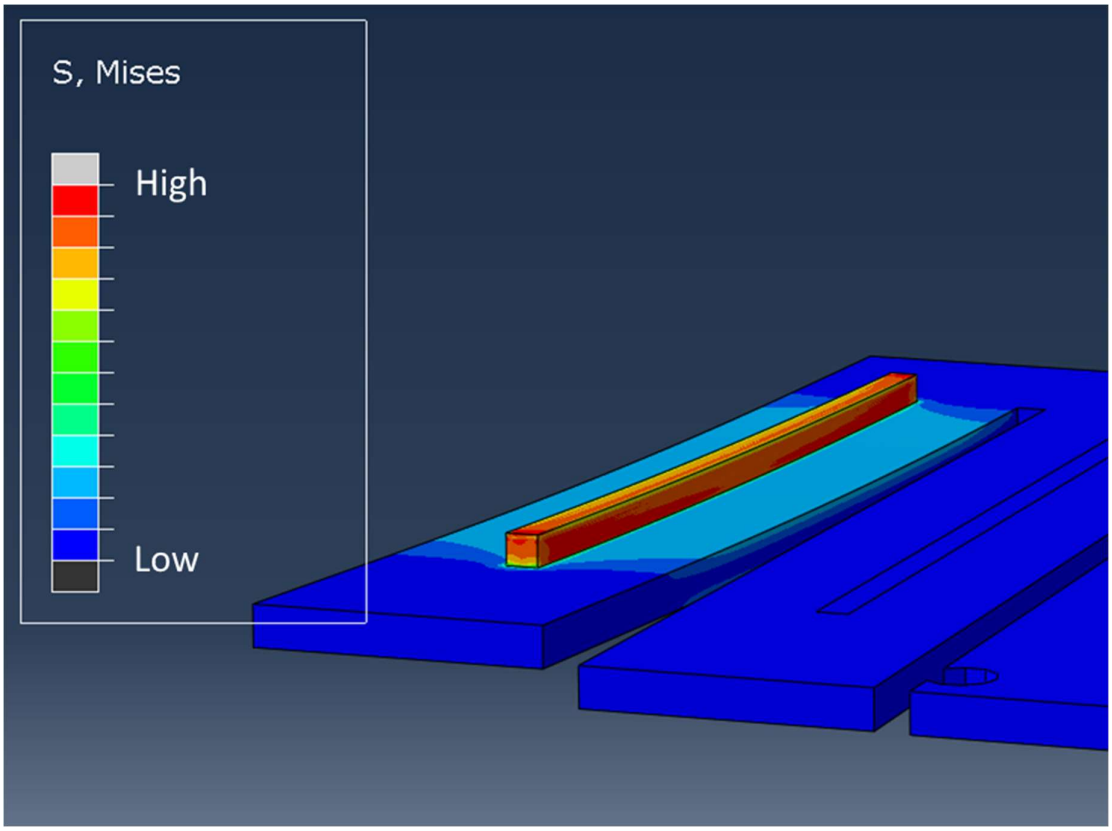

Figure 9: Example result of the FE analysis of a cantilever print. It shows the internal stress in the print and the base plate, and also the distortion of the cantilever.

3.3 Mechanical multi-material calibration

The results of the multi-material print exhibit similar distortion patterns and magnitudes when compared to the uni-material prints. The distortion observed in the multi-material prints follows a similar order of magnitude and trend. These findings are illustrated in Figure 10, which presents the curvatures of the baseplate resulting from the print. The figure also includes the results from the uni-material print for comparison. In the case of the uni-material print, it can be observed that the experimental results indicate higher levels of distortion compared to the Finite Element Analysis (FEA) results. However, the overall trend and similarity between the experimental and FEA results suggest that the FEA model captures the fundamental deformation behaviour. Fine-tuning and calibration of certain simulation parameters could potentially bring the simulated and experimental distortions into closer agreement. These findings demonstrate the potential of the FEA model to predict and simulate the distortion patterns in both uni-material and multi-material prints. The overall agreement between the experimental and simulated results provides confidence in the accuracy and reliability of the FEA model in capturing the deformation behaviour of the printed components.

It is notable that the multi-material case exhibits a discrepancy, wherein the model overestimates the distortion of the cantilevers, compared to the uni-material case. This contradiction poses a challenge as it implies that calibrating the results using arbitrary simulation parameters would lead to either overestimation or underestimation in one of the cases. In this situation, attempting to calibrate the simulation parameters to improve accuracy in one case would likely exacerbate the divergence in the other case.

This means obtaining accurate results using this modelling technique is inherently dependent on the material properties. The material properties play a crucial role in calibrating the models to faithfully represent the experimental observations. It is evident that the modelling technique's accuracy relies on accounting for the specific material properties involved. Utilizing these properties for model calibration is essential for achieving accurate predictions and comprehending the intricate relationships between material properties, process parameters, and resulting deformations. In conclusion, the simulated deformative behaviour is largely in agreement with the experimental observations. Acknowledging the influence of material properties and utilizing them for model calibration is indispensable for obtaining precise results and ensuring that the modelling technique effectively captures the experimental reality.

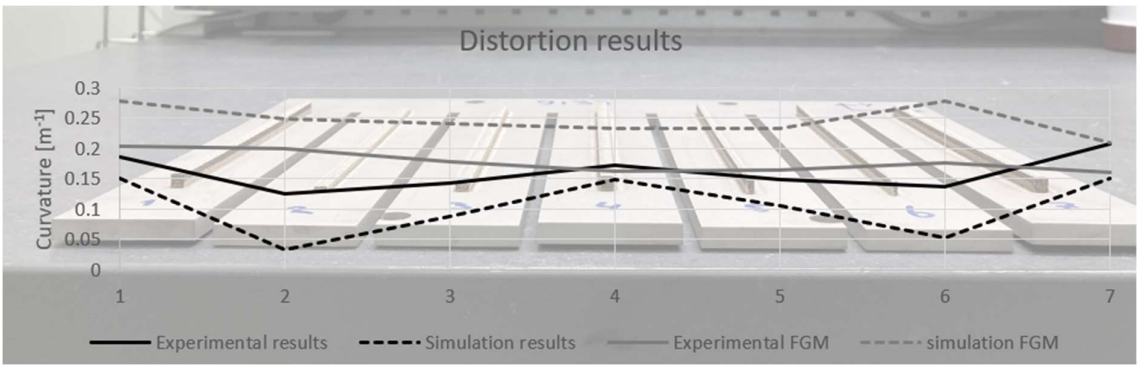

Figure 10: Combined distortion results of the geometric (uni-material) and multi-material cantilevers. It shows the measured curvature of the cantilevers and the simulated curvature.

4 CONCLUSIONS AND RECOMMENDATIONS

This research presents a modelling technique capable of simulating a DED print on a part-scale, encompassing both thermal and mechanical aspects. The key findings and conclusions are as follows:

- The thermal physics can be accurately represented using this method, with the exception of the intricate physics associated with the melt pool.
- The mechanical physics, including internal stresses and distortion, can be accurately represented to a certain extent. It is emphasized that calibration using material properties is essential for improving the accuracy of the mechanical models.
- The research demonstrates the capability of the method to simulate multi-material prints and functional gradient prints, expanding its applicability to diverse printing scenarios.

Based on these findings, the following recommendations are made:

- The method should undergo validation through demonstrator prints to assess its accuracy and determine the necessity for further calibration.
- Validation of the thermal models should involve larger structures rather than solely thin walls to ensure their robustness and reliability.
- Further research is required to investigate the impact of simulation parameters on the results, aiming to refine and optimize the modelling process.

Implementing these recommendations will enhance the understanding and applicability of the modelling technique, paving the way for more accurate and reliable simulations of DED prints on a larger scale.

REFERENCES

[1] Piscopo, G., Atzeni, E., Salmi, A., 2019. *A Hybrid Modeling of the Physics-Driven Evolution of Material Addition and Track Generation in Laser Powder Directed Energy Deposition.* Materials 12, 2819

[2] Michael E. Stender, Lauren L. Beghini, Joshua D. Sugar, Michael G. Veilleux, Samuel R. Subia, Thale R. Smith, Christopher W. San Marchi, Arthur A. Brown, Daryl J. Dagel. *A thermal-mechanical finite element workflow for directed energy deposition additive manufacturing process modeling.* Additive Manufacturing, Volume 21, (2018) Pages 556-566

[3] Parnian Kiani, Alexander D. Dupuy, Kaka Ma, Julie M. Schoenung, *Directed energy deposition of AlSi10Mg: Single track nonscalability and bulk properties*, Materials & Design, Volume 194, (2020) 108847

[4] E.S. Puchi Cabrera, ‘*’High temperature deformation of 316L stainless steel’’*, Materials Science and Technology, 17:2, 155-161

[5] K. Yuan, W. Guo, P. Li, Y. Zhang, X. Li, and X. Lin, *“Thermomechanical behavior of laser metal deposited inconel 718 superalloy over a wide range of temperature and strain rate: Testing and constitutive modeling,”* Mechanics of Materials, vol. 135, p. 13–25, (2019)